

## SINGLE-TONE FREQUENCY ESTIMATION BASED ON REFORMED COVARIANCE FOR HALF-LENGTH AUTOCORRELATION

Sergiusz Sienkowski, Mariusz Krajewski

University of Zielona Góra, Institute of Metrology, Electronics and Computer Science, Szafrana 2, 65-516 Zielona Góra, Poland (✉ [s.sienkowski@imei.uz.zgora.pl](mailto:s.sienkowski@imei.uz.zgora.pl), +48 68 328 26 78, [m.krajewski@imei.uz.zgora.pl](mailto:m.krajewski@imei.uz.zgora.pl))

### Abstract

This paper presents a new simple and accurate frequency estimator of a sinusoidal signal based on the signal autocorrelation function (ACF). Such an estimator was termed as the reformed covariance for half-length autocorrelation (RC-HLA). The designed estimator was compared with frequency estimators well-known from the literature, such as the modified covariance for half-length autocorrelation (MC-HLA), reformed Pisarenko harmonic decomposition for half-length autocorrelation (RPHD-HLA), modified Pisarenko harmonic decomposition for half-length autocorrelation (MPHD-HLA), zero-crossing (ZC), and iterative interpolated DFT (IpDFT-IR) estimators. We determined the samples of the ACF of a sinusoidal signal disturbed by Gaussian noise (simulations studies) and the samples of the ACF of a sinusoidal voltage (experimental studies), calculated estimators based on the obtained samples, and computed the mean squared error (MSE) to compare the estimators. The errors were juxtaposed with the Cramér–Rao lower bound (CRLB). The research results have shown that the proposed estimator is one of the most accurate, especially for  $\text{SNR} > 25$  dB. Then the RC-HLA estimator errors are comparable to the MPHD-HLA estimator errors. However, the biggest advantage of the developed estimator is the ability to quickly and accurately determine the frequency based on samples collected from no more than five signal periods. In this case, the RC-HLA estimator is the most accurate of the estimators tested.

Keywords: frequency estimator, sinusoidal signal, autocorrelation function, mean squared error.

© 2020 Polish Academy of Sciences. All rights reserved

## 1. Introduction

This paper investigates the problem of single-tone signal frequency estimation. Such a signal is called a sinusoidal signal. This class of signal with noise is measured in radar [1] and sonar [2] technologies, wireless communications [3], and speech signal analysis [4]. For this reason, this paper concerns the study of frequency estimators carried out for a model of a sinusoidal signal disturbed by Gaussian noise, like in [5–16].

Various frequency estimators of a sinusoidal signal have been designed over the years. An important group of time-discrete frequency estimators calculated in the time domain based on signal samples or *signal autocorrelation function* (ACF) samples has been developed. The most

well-known member of this group of estimators is the *modified covariance* (MC) [5] estimator which can be calculated based on any number of consecutive sinusoidal signal samples. A special case of the MC estimator is the aforementioned three-point estimator [5–12]. Such an estimator follows from the equation of linear signal sample prediction [17]. If the signal samples in the MC estimator are replaced with samples of the ACF of the signal, then a correlation frequency estimator known as the *modified covariance for correlation* (MCC), is obtained [10, 11]. If the MCC is calculated on the basis of half of the number of the ACF samples, it is called the MC-HLA (*modified covariance for half-length autocorrelation*) [12]. Both estimators offer a highly accurate frequency estimation due to which it is often compared with other sinusoidal signal frequency estimators. Apart from the MCC estimator, there are various other estimators calculated based on either the samples of the ACF or its components. Particular focus should be on the *Pisarenko harmonic decomposition* (PHD) estimator. Pisarenko observed that the eigenvalues and eigenvector of the matrix of ACF samples could be used to estimate the frequency. This laid the foundation for the design of a sinusoidal signal estimator calculated based on two samples of the signal ACF [18]. In subsequent years, a few important modifications of the PHD estimator were developed such as the reformed *Pisarenko harmonic decomposition* (RPHD) [13] and *modified Pisarenko harmonic decomposition* (MPHD) [14] estimators. If the RPHD and MPHD are calculated with the HLA, then they are called the RPHD-HLA and MPHD-HLA, respectively [12]. In addition to the estimators listed, the time-discrete *zero-crossing* (ZC) estimators are also noteworthy [19]. The ZC estimators use the zero crossings of a sinusoidal signal for frequency estimation. In this paper, for comparative studies, the ZC estimator with linear interpolation of signal samples at the zero crossing point was used [1]. The ZC estimators are sensitive to noise that occurs in the signal. Therefore, pre-filtering of the signal is often performed before using the ZC estimators. One of the effects of this is an increasing the SNR (*signal-to-noise ratio*) level. No filters were used in estimators tests presented in the paper, but simulations and experiments were also performed with high SNR.

Furthermore, besides the estimators calculated in the time domain, there is also a group of estimators calculated in the frequency domain such as the popular IpDFT (interpolated DFT). Such estimators are calculated based on the harmonics of the DFT spectrum of a signal [20–26]. Nowadays, the possibility of obtaining high accuracy frequency estimation is offered by the IpDFT iterative algorithms [22–26]. One of the newest and most accurate is the IpDFT-IR algorithm developed by Belega, Petri and Dallet [26], which was applied in this paper for comparative studies.

This paper presents a new simple and accurate frequency estimator of a sinusoidal signal based on the ACF. Such an estimator is termed as the *reformed covariance for half-length autocorrelation* (RC-HLA). Section 2 presents the mathematical model of a sinusoidal signal disturbed by additive Gaussian noise, whose frequency was estimated using the designed estimator. Section 2 also presents the ACF and its properties which were later applied to determine the theoretical *mean square error* (MSE) of the RC-HLA estimator. Section 3 presents the RC-HLA estimator and its properties and the MSEs of the RC-HLA frequency estimation obtained by simulations and experimental studies. These errors were juxtaposed with the errors corresponding to the selected MC-HLA, RPHD-HLA, MPHD-HLA, ZC, and IpDFT-IR estimators and the *Cramér–Rao lower bound* (CRLB). The research results have shown that the proposed estimator is one of the most accurate, especially for SNR > 25 dB. Then the RC-HLA estimator errors are comparable to the MPHD-HLA estimator errors. However, the biggest advantage of the developed estimator is the ability to quickly and accurately determine the frequency based on samples collected from no more than five signal periods. In this case, the RC-HLA estimator is the most accurate of the

estimators tested. Section 3 also presents computational complexities of the analyzed estimators, while Section 4 summarizes the research results. One appendix related to Section 3 can be found at the end.

## 2. Signal autocorrelation function and its properties

Let  $y(t)$  be the sum of a sinusoidal signal  $x(t)$  with amplitude  $A$ , frequency  $f$ , angular frequency  $\omega_0 \in (0, \pi)$ , initial phase  $\varphi \in [0, 2\pi)$ , and additive Gaussian noise  $q(t)$  with a zero mean value  $\mu_q$  and standard deviation  $\sigma_q$ . If  $y(t)$  is sampled at a sampling frequency  $f_s$ , then its samples can be described by the formula:

$$y[n] = x[n] + q[n], \quad n = 0 \dots 2M - 1, \quad (1)$$

where

$$x[n] = A \sin(\omega_0 n + \varphi) \quad (2)$$

and  $q[n]$  are the samples of the signal  $x(t)$  and noise  $q(t)$ , respectively. Significant relationships exist between  $\omega_0$ ,  $f$ , and  $f_s$  as detailed below:

$$\omega_0 = 2\pi \frac{f}{f_s}, \quad f_s = \frac{2M}{N} f, \quad (3)$$

where  $N$  represent the number of periods of the signal  $x(t)$ .

Let  $R(s, \tau)$  represent the ACF of the signal  $s(t)$  occurring in the form of a periodic signal, random signal(noise), or sum of both signals. Samples of the ACF of the signal  $s(t)$  can be determined by applying the formula

$$\tilde{R}[s, k] = \frac{1}{M} \sum_{n=0}^{M-1} s[n] s[n+k], \quad k = 0 \dots M - 1. \quad (4)$$

Formula (4) is an half-length estimator of the ACF calculated based on the samples  $s[n]$  of the signal  $s(t)$ , and the samples  $s[n+k]$  of its copy  $s(t + \tau)$  delayed by time  $\tau$  [27].

The results of the estimation of the function  $R(s, \tau)$  can be evaluated based on the mean square error

$$\text{MSE} [\tilde{R}[s, k]] = \text{Var} [\tilde{R}[s, k]] + b^2 [\tilde{R}[s, k]] \quad (5)$$

of the estimator  $\tilde{R}[s, k]$ . This error results from the bias

$$b [\tilde{R}[s, k]] = E [\tilde{R}[s, k]] - R(s, \tau) \quad (6)$$

and variance

$$\text{Var} [\tilde{R}[s, k]] = E [\tilde{R}^2 [s, k]] - E^2 [\tilde{R}[s, k]] \quad (7)$$

of the estimator, where  $E[\cdot]$  is the expected value operator.

If  $s(t)$  is the sinusoidal signal  $x(t)$ , then by substituting (2) in (4) the following formula can be obtained

$$\tilde{R}[x, k] = \frac{1}{M} \sum_{n=0}^{M-1} x[n]x[n+k] = \frac{A^2}{2} \cos(k\omega_0) + \rho(k), \quad (8)$$

where

$$\rho(k) = \frac{A^2 \sin((k-1)\omega_0 + 2\varphi) - \sin((2M+k-1)\omega_0 + 2\varphi)}{4M \sin(\omega_0)}. \tag{9}$$

As

$$R(x, \tau) = \frac{1}{T} \int_0^T x(t)x(t+\tau) dt = \frac{A^2}{2} \cos\left(\frac{2\pi}{T}\tau\right), \quad T = \frac{1}{f}, \tag{10}$$

then

$$\tilde{R}[x, k] = R(x, k \cdot T_s) + \rho(k), \quad T_s = \frac{1}{f_s}. \tag{11}$$

The expected value and variance of the estimator  $\tilde{R}[x, k]$  are given by

$$E[\tilde{R}[x, k]] = R(x, k \cdot T_s) + \rho(k), \quad \text{Var}[\tilde{R}[x, k]] = 0. \tag{12}$$

Based on (5)–(7), (10) and (12), we obtain

$$\text{MSE}[\tilde{R}[x, k]] = \rho^2(k). \tag{13}$$

If  $s(t)$  is the signal  $y(t)$ , then

$$\begin{aligned} \tilde{R}[y, k] &= \frac{1}{M} \sum_{n=0}^{M-1} y[n]y[n+k] \\ &= \tilde{R}[x, k] + \tilde{R}[q, k] + \frac{1}{M} \sum_{n=0}^{M-1} (x[n]q[n+k]) + \frac{1}{M} \sum_{n=0}^{M-1} (x[n+k]q[n]) \end{aligned} \tag{14}$$

and

$$\begin{aligned} E[\tilde{R}[y, k]] &= \begin{cases} \tilde{R}[x, 0] + \sigma_q^2, & k = 0, \\ \tilde{R}[x, k], & k > 0, \end{cases} \\ \text{Var}[\tilde{R}[y, k]] &= \begin{cases} \frac{2\sigma_q^4}{M} + \frac{4\sigma_q^2}{M} \tilde{R}[x, 0], & k = 0, \\ \frac{\sigma_q^4}{M} + \frac{2\sigma_q^2}{M} \tilde{R}[x, 0] + \frac{2\sigma_q^2}{M^2} (M-k) \tilde{R}[x, 2k], & k > 0. \end{cases} \end{aligned} \tag{15}$$

Then

$$\text{MSE}[\tilde{R}[y, k]] = \begin{cases} \frac{2\sigma_q^4}{M} + \frac{4\sigma_q^2}{M} \tilde{R}[x, 0] + (\tilde{R}[x, 0] + \sigma_q^2 - R(x, 0))^2, & k = 0, \\ \frac{\sigma_q^4}{M} + \frac{2\sigma_q^2}{M} \tilde{R}[x, 0] + \frac{2\sigma_q^2}{M^2} (M-k) \tilde{R}[x, 2k] + (\tilde{R}[x, k] - R(x, k \cdot T_s))^2, & k > 0. \end{cases} \tag{16}$$

Formula (15) was derived based on [12, 27, 28]. Unlike formulas known from the literature, it allows determining the expected value and variance of the estimator  $\tilde{R}[y, 0]$  (mean squared value) taking into account the component (9) influence. The presented properties of the  $\tilde{R}[y, k]$  estimator were employed while evaluating the developed RC-HLA frequency estimator.

### 3. RC-HLA frequency estimator

#### 3.1. The estimator and its properties

Let  $m$  and  $w$  be such that  $3 \leq m \leq M$  and  $0 \leq w \leq m-3$ . Then the angular frequency  $\omega_0$  of the signal  $x(t)$  can be calculated based on the samples  $\tilde{R}[y, k]$  of the autocorrelation function  $R(x, \tau)$  of the signal  $x(t)$  using the formula

$$\omega_0 = \cos^{-1} \left( \frac{C_1}{2C_2} \right), \quad (17)$$

where

$$C_1 = \sum_{k=1}^{m-w-2} \sum_{n=0}^w a(x, n+k) r(x, n+k), \quad C_2 = \frac{1}{2} \sum_{k=1}^{m-w-2} \sum_{n=0}^w a(x, n+k), \quad (18)$$

and

$$a(x, k) = \tilde{R}^2[x, k], \quad r(x, k) = \frac{\tilde{R}[x, k-1] + \tilde{R}[x, k+1]}{2\tilde{R}[x, k]}. \quad (19)$$

Formula (17) results directly from model 3 of the frequency estimation proposed by Adelson in [5]. From this model it follows that if we consider the expressions  $r(x, 1)$  and  $r(x, 2)$  and assume such expressions to be uncorrelated, then  $\cos(\omega_0) = C_1/(2C_2)$ , where  $C_1 = a \cdot r(x, 1) + b \cdot r(x, 2)$ ,  $C_2 = (a + b)/2$ , with  $a = a(x, 1)$  and  $b = a(x, 2)$ . If we develop the coefficients  $C_1$  and  $C_2$  into finite sums with the limit  $w$  (internal sums from formula (18)) and apply a generalization of the Vizireanu estimator [6] to the MC-HLA estimator [12] (external sums from formula (18)), we can obtain the final form of the presented formula after determining the inverse function of  $\cos(\cdot)$ .

Let us assume without loss of generality that  $m = M$ . If we substitute the samples  $\tilde{R}[x, k]$  with the samples  $\tilde{R}[y, k]$  of the autocorrelation function  $R(y, \tau)$  of the signal  $y(t)$ , then

$$\tilde{\omega}_0^{\text{RC-HLA}} = \cos^{-1} \left( \frac{C_1}{2C_2} \right), \quad (20)$$

would be an estimator of the angular frequency  $\omega_0$ , where

$$C_1 = \sum_{k=1}^{M-w-2} \sum_{n=0}^w a(y, n+k) r(y, n+k), \quad (21)$$

$$C_2 = \frac{1}{2} \sum_{k=1}^{M-w-2} \sum_{n=0}^w a(y, n+k),$$

and

$$a(y, k) = \tilde{R}^2[y, k], \quad r(y, k) = \frac{\tilde{R}[y, k-1] + \tilde{R}[y, k+1]}{2\tilde{R}[y, k]}. \quad (22)$$

We shall term estimator (20) as the RC-HLA (reformed covariance for half-length autocorrelation).

It can easily be noted that if we assume  $M = 3$  in (20), then

$$\tilde{\omega}_0^{\text{RC-HLA}} = \cos^{-1} (r(y, 1)). \quad (23)$$

We can thus obtain an instantaneous estimator corresponding/similar to a three-point estimator of the angular frequency  $\omega_0$  presented previously for *e.g.* in Vizireanu’s works [6]. If the parameter  $w$  in (20) is equal to zero ( $w = 0$ ), then the RC-HLA assumes the form

$$\tilde{\omega}_0^{\text{RC-HLA}} = \tilde{\omega}_0^{\text{MC-HLA}} = \cos^{-1} \left( \frac{C_1}{2C_2} \right), \tag{24}$$

where

$$C_1 = \sum_{k=1}^{M-2} a(y, k) r(y, k), \quad C_2 = \frac{1}{2} \sum_{k=1}^{M-2} a(y, k). \tag{25}$$

Estimator (24) is known as the MC-HLA [12]. Thus, the MC-HLA is a special case of the RC-HLA estimator. It can be noted that if  $M - w = 3$ , then both the RC-HLA and MC-HLA yield the same results when estimating the angular frequency  $\omega_0$ . Moreover, if  $M = 3$  and  $w = 1$  in (20), another special case of the RC-HLA estimator can be obtained that corresponds to the one presented by Adelson in [5].

One of the most important terms of the RC-HLA estimator is the parameter  $w$ . Various studies have investigated the effect of the parameter  $w$  on the accuracy achieved when estimating the angular frequency  $\omega_0$ . For this purpose, estimator errors

$$\tilde{\text{MSE}} \left[ \tilde{\omega}_0^{\text{RC-HLA}} \right] = \frac{1}{K} \sum_{j=0}^{K-1} \left( \tilde{\omega}_0^{\text{RC-HLA}} [j] - \omega_0 \right)^2 \tag{26}$$

in the function  $w$  were determined where  $K$  is the repetitions number of the angular frequency estimation  $\omega_0$ . The results indicated that selecting an appropriate parameter value is critical when  $M$  is large and the SNR ( $\text{SNR} = 10 \cdot \log(0.5A^2/\sigma_q^2)$ ) is small and positive (*e.g.* SNR = 10 dB). We can then assume that  $w \ll M$  markedly increases the accuracy of the results when estimating  $\omega_0$ . The maximum accuracy was predominantly obtained when  $3 \leq \tilde{w} \leq 5$ , where

$$\tilde{w} = \underset{0 \leq w \leq M-3}{\text{argmin}} \left\{ \tilde{\text{MSE}} \left[ \tilde{\omega}_0^{\text{RC-HLA}} \right] \right\}. \tag{27}$$

The authors recommend selecting  $w = \tilde{w} = 5$  in this situation. The same  $w$  value is also recommended for other measurement conditions. In cases where  $M - \tilde{w} < 3$ ,  $w = 1$  should be assumed.

Researching the probabilistic properties of estimators belonging to the MCC (also MC-HLA) class is a complex task. A few researchers have proposed mathematical formulae to calculate the MSE of the estimators with good approximation [10–12, 14, 15]. However, the developed formulae are often complicated. Formulae are usually developed by using Taylor’s series to expand the expressions for random variable function moments [29, 30]. On this basis, an approximation of the RC-HLA estimator MSE was determined. In deriving the formula for theoretical MSE, it was assumed without loss of generality that the component (9) is negligible.

If  $w = 5$ , then the MSE of the RC-HLA estimator can be determined from the formula (see Appendix)

$$\text{MSE} \left[ \tilde{\omega}_0^{\text{RC-HLA}} \right] \approx \frac{\mathbf{h}^T \mathbf{D} \mathbf{h}}{9A^4 (M - 7)^2 \sin^2(\omega_0)}, \tag{28}$$

where  $\mathbf{D}$  is a covariance matrix with size  $M \times M$  and elements  $d_{k,m}$ ,  $k, m = 1 \dots M$ , while  $\mathbf{h}$  is a vector with size  $M \times 1$  and elements  $h_i$ ,  $i = 1 \dots M$ . The elements  $d_{k,m}$  and  $h_i$  can be described by formulas (34) and (45).

Based on (28), MSE characteristics of the RC-HLA estimator as a function of the SNR,  $M$ , and  $N$  were determined (Fig. 1). We set  $A = 2$  V,  $w = 5$ , and  $K = 1000$  in the simulations. The phase  $\varphi$  was randomized using a pseudo-random number generator with uniform distribution

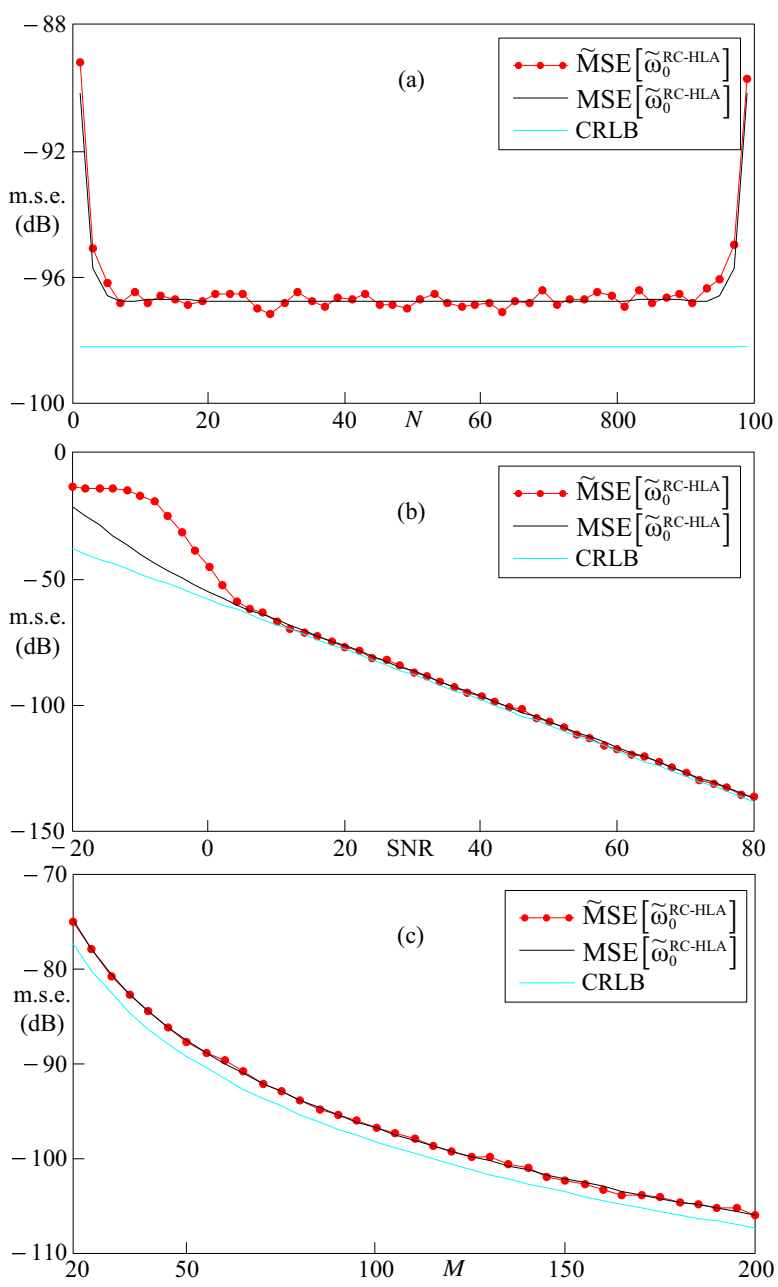


Fig. 1. Results showing the MSE and  $\tilde{\text{MSE}}$  of the RC-HLA estimator as functions of the  $N$ , SNR, and  $M$  for  $w = 5$ , and  $K = 1000$ . (a)  $0.01 \leq \omega_0/\pi \leq 0.99$ ,  $M = 100$ , SNR = 40 dB, (b)  $\omega_0/\pi = 0.5$ ,  $N = 50$ ,  $M = 100$ , and (c)  $\omega_0/\pi = 0.5$ , SNR = 40 dB.

in the range  $[0, 2\pi]$ . To verify the MSE results, the estimator  $\widetilde{\text{MSE}}$  of the MSE was also calculated based on the  $K$  results obtained from estimating the angular frequency  $\omega_0$ . The MSE and  $\widetilde{\text{MSE}}$  results were juxtaposed with the calculated CRLB based on the formula [31]

$$\text{CRLB} \approx \frac{12}{10^{\frac{\text{SNR}}{10}} (2M) (4M^2 - 1)}. \quad (29)$$

Research shows that if the SNR is large, then  $\text{MSE} \approx \widetilde{\text{MSE}}$ . This proves that formula (28) would be useful for a large SNR which is consistent with the results of similar analyses presented for *e.g.* in [10–12]. Moreover, the MSE and  $\widetilde{\text{MSE}}$  depend on the variance to a greater degree than the bias of the estimator when the SNR has a large, positive value.

### 3.2. Simulation studies

Various studies have focused on estimating the angular frequency  $\omega_0$  by applying the RC-HLA along with other estimators such as the MC-HLA, RPHD-HLA, MPHD-HLA [12], ZC [1], and IpDFT-IR [26]. The  $\widetilde{\text{MSE}}$  of the estimators has been determined and compared for various  $N$  (or  $\omega_0/\pi$ ), SNR, and  $M$  values. We set  $A = 2$  V,  $w = 5$ , and  $K = 1000$  in the simulations. Nevertheless, it should be taken into account that in case of the ACF-based estimators the signal amplitude  $A$  does not affect of the  $\widetilde{\text{MSE}}$ . On the other hand, assuming the number of repetitions  $K$  above 100 allows obtaining high repeatability of the research results. The initial phase was randomized during the simulations using a pseudo-random number generator with a uniform distribution over the range  $[0, 2\pi]$ . The IpDFT-IR estimator was calculated in three iterations. The MSE results were juxtaposed with the CRLB. The mean deviations

$$\bar{\Delta} = \frac{1}{W} \sum_{k=0}^{W-1} (\widetilde{\text{MSE}}[\tilde{\omega}_0, k] - \text{CRLB}[k]) \quad (30)$$

of the  $\widetilde{\text{MSE}}$  values of each estimator from the CRLB values were determined for each  $\widetilde{\text{MSE}}$  characteristic, where  $W$  is the number of points on the  $\widetilde{\text{MSE}}$  characteristic. The research results are presented and discussed in three sections.

#### 3.2.1. Estimation errors as a function of number of periods

Examples of measurement situations have been considered for  $0.005 \leq \omega_0/\pi \leq 0.05$  and  $0.01 \leq \omega_0/\pi \leq 0.99$ . From (3) it follows that the first situation we deal with a small number of signal periods, *i.e.*  $0.5 \leq N \leq 5$  (Figs. 2a and 2b). In the second situation, the MSE results were presented in a wide range of  $1 \leq N \leq 99$  (Figs. 3a and 3b). All the studies were carried out for  $M = 100$ . The obtained results have shown that if  $N < 5$ , then the RC-HLA estimator is the most accurate. This is confirmed by the  $\bar{\Delta}$  results presented in Table 1. For example, if  $\text{SNR} = 40$  dB, then the RC-HLA estimator is more accurate than the MPHD-HLA, MC-HLA, RPHD-HLA, IpDFT-IR and ZC estimators by 1.08, 4.41, 4.45, 5.85, and 9.75 dB, respectively. The obtained results (Table 1) shows that if  $N > 5$ , then the RC-HLA and MPHD-HLA estimators have a comparable accuracy. However, they are more accurate than the other estimators that use the ACF by around 0.5 dB and more accurate than the ZC and IpDFT-IR estimators by around 32 and 7 dB for  $\text{SNR} = 40$  dB, respectively.



Table 1. The results of deviations  $\bar{\Delta}$  [dB] obtained on the basis of data from Figs. 2 and 3.

$N(\omega_0/\pi)$	SNR [dB]	MC-HLA	RPHD-HLA	MPHD-HLA	RC-HLA	ZC	IpDFT-IR
$0.5 \leq N \leq 5$ ( $0.005 \leq \omega_0/\pi \leq 0.05$ )	40	8.86	8.90	5.53	4.45	14.2	10.3
$0.5 \leq N \leq 5$ ( $0.005 \leq \omega_0/\pi \leq 0.05$ )	70	8.00	8.00	5.52	4.34	14.3	31.9
$1 \leq N \leq 99$ ( $0.01 \leq \omega_0/\pi \leq 0.99$ )	40	2.53	2.53	2.02	1.89	34.3	9.03
$1 \leq N \leq 99$ ( $0.01 \leq \omega_0/\pi \leq 0.99$ )	70	2.44	2.44	2.06	1.94	59.5	11.5

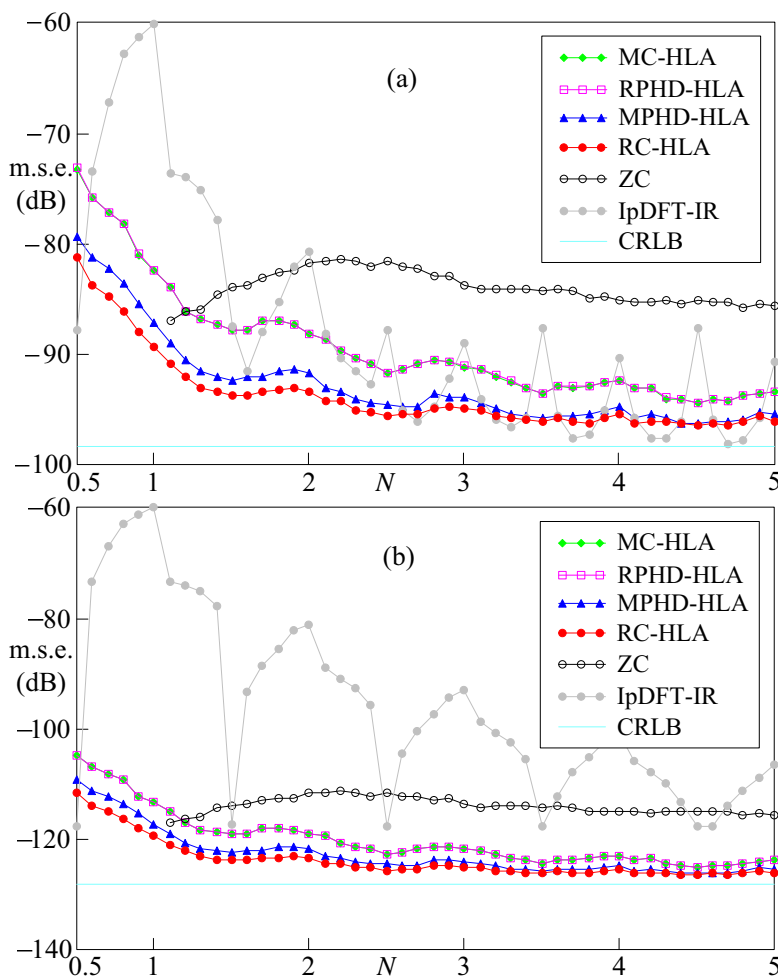


Fig. 2. Results showing the  $\bar{MSE}$  as a function of  $N$  for  $0.005 \leq \omega_0/\pi \leq 0.05$ ,  $M = 100$ ,  $w = 5$ , and  $K = 1000$ . (a) SNR = 40 dB, and (b) SNR = 70 dB.

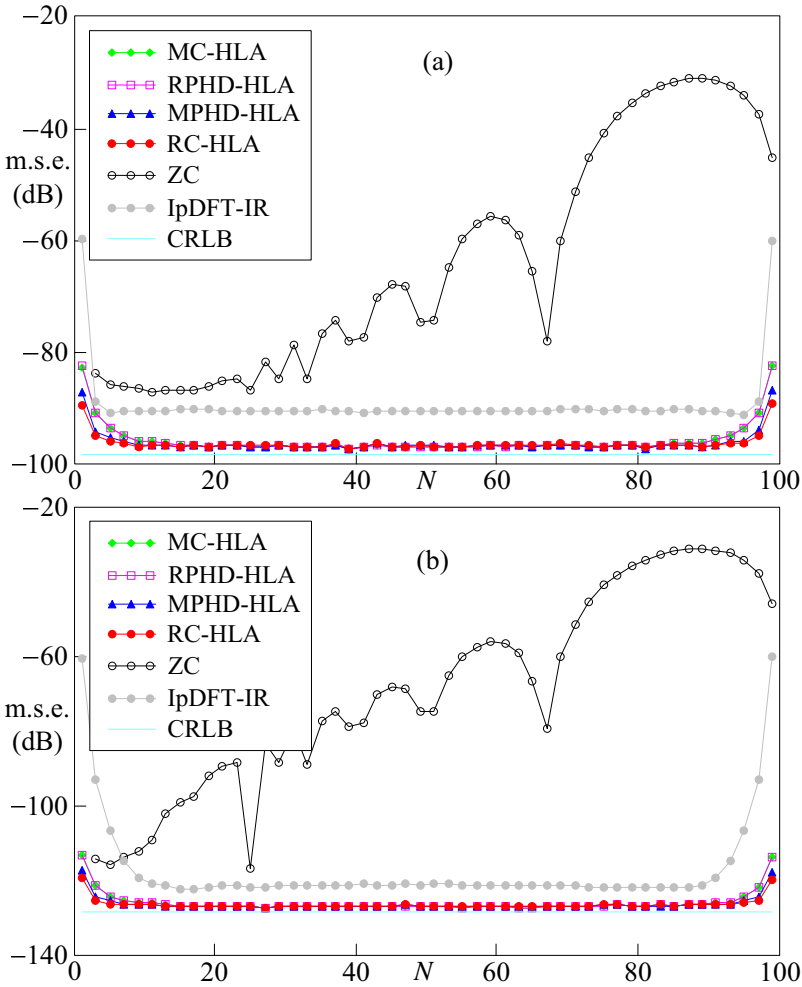


Fig. 3. Results showing the  $\tilde{MSE}$  as a function of  $N$  for  $0.01 \leq \omega_0/\pi \leq 0.99$ ,  $M = 100$ ,  $w = 5$ , and  $K = 1000$ .(a) SNR = 40 dB, and(b) SNR = 70 dB.

### 3.2.2. Estimation errors as a function of SNR

Examples of measurement situations have been considered for  $N = 2$  (Fig. 4a) and  $N = 50$  (Fig. 4b). The research results have shown that the RC-HLA estimator is characterized by the highest accuracy when  $SNR > 25$  dB and  $N$  is small. For example, if  $N = 2$ , then the differences between the mean deviation  $\bar{\Delta}$  of the RC-HLA estimator and the mean deviations  $\bar{\Delta}$  of the MPHD-HLA, MC-HLA, RPHD-HLA, ZC and IpDFT-IR estimators are equal to 1.45, 5.76, 5.76, 20.3, and 25.8 dB, respectively (Table 2). If  $SNR > 25$  dB and  $N$  is large, then the RC-HLA estimator is less accurate than the MC-HLA and RPHD-HLA estimators *e.g.* for  $N = 50$  by around 0.1 dB. In the same measurement conditions, the RC-HLA and MPHD-HLA estimators are more accurate than the ZC and IpDFT-IR estimators by around 11 and 6 dB, respectively.

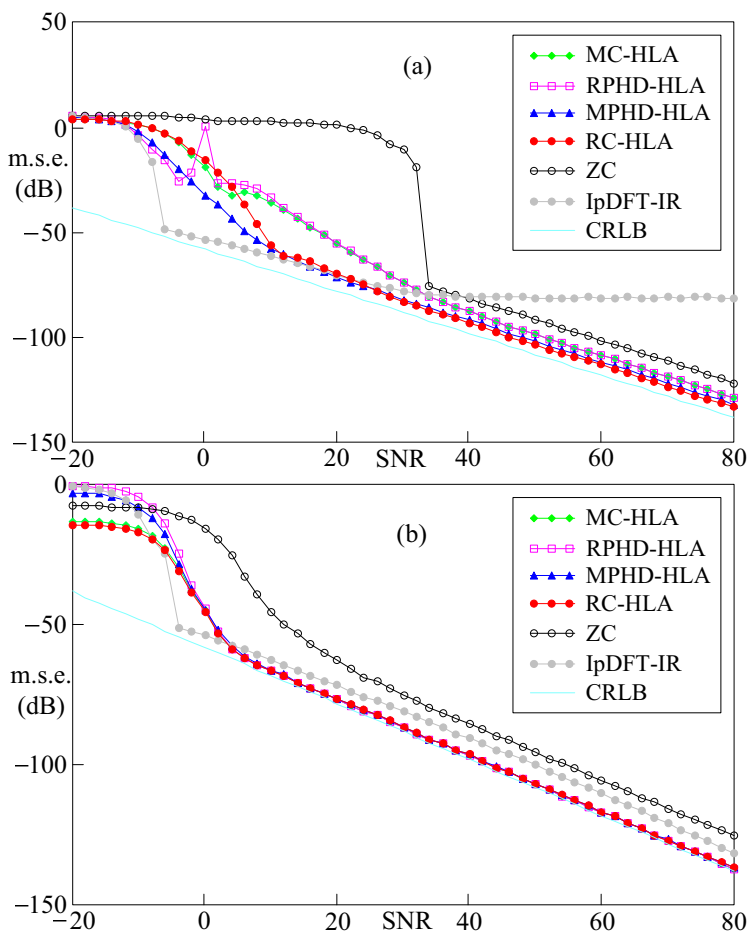


Fig. 4. Results showing the  $\tilde{\text{MSE}}$  as a function of  $\text{SNR}$  for  $M = 100$ ,  $w = 5$ , and  $K = 1000$ . (a)  $\omega_0/\pi = 0.02$ ,  $N = 2$ , and (b)  $\omega_0/\pi = 0.5$ ,  $N = 50$ .

Table 2. The results of deviations  $\bar{\Delta}$  [dB] obtained on the basis of data from Fig. 4.

$N(\omega_0/\pi)$	SNR [dB]	MC-HLA	RPHD-HLA	MPHD-HLA	RC-HLA	ZC	IpDFT-IR
2(0.02)	-20÷80	22.2	22.5	14.7	16.4	43.5	24.8
2(0.02)	26÷80	10.6	10.6	6.29	4.84	25.1	30.6
50(0.5)	-20÷80	6.92	8.87	8.48	6.77	20.7	11.4
50(0.5)	26÷80	1.37	1.37	1.54	1.49	12.7	7.49

### 3.2.3. Estimation errors as a function of number of samples

Examples of measurement situations have been considered when  $10 \leq M \leq 200$  for  $\omega_0/\pi = 0.01$  (Fig. 5a) and  $\omega_0/\pi = 0.5$  (Fig. 5b). The research results have shown that if  $\text{SNR} = 40$  dB and  $\omega_0/\pi = 0.5$ , then the RC-HLA estimator has a mean deviation  $\bar{\Delta}$  equal to around 1.5 dB,

similar to the deviations of the other estimators that use the ACF. The RC-HLA estimator is the most accurate when  $\text{SNR} = 40 \text{ dB}$  and  $\omega_0/\pi = 0.01$ . Then the differences between the mean deviation  $\bar{\Delta}$  of the RC-HLA estimator, and the mean deviations  $\bar{\Delta}$  of the MPHD-HLA, ZC, MC-HLA, RPHD-HLA, and IpDFT-IR estimators are equal to 2, 4.9, 6.9, 6.9, and 19.3 dB, respectively (Table 3).

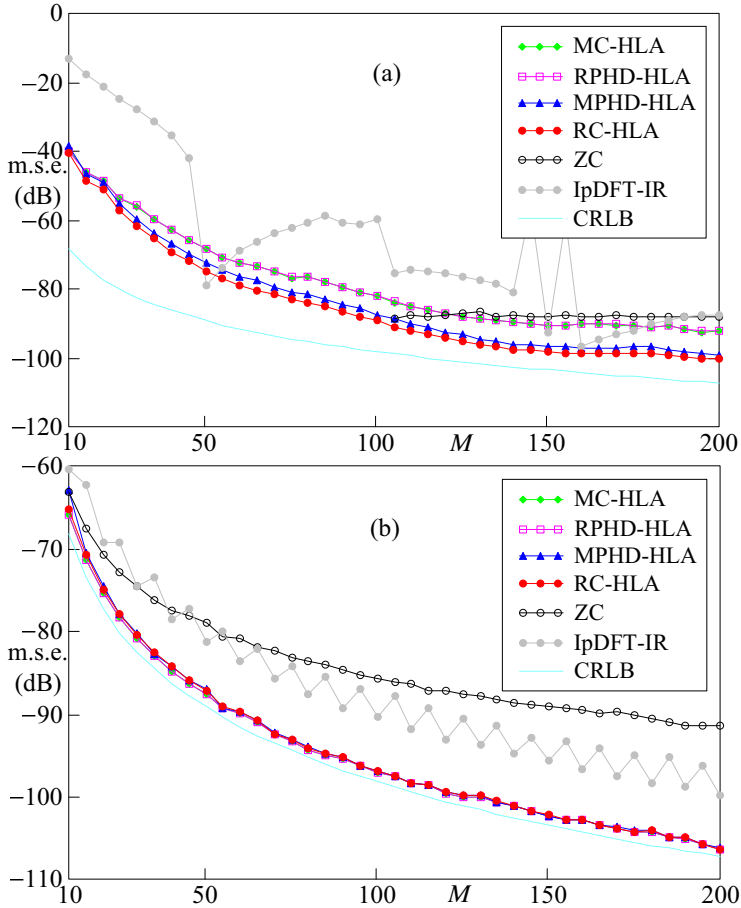


Fig. 5. Results showing the  $\bar{\text{MSE}}$  as a function of  $M$  for  $w = 5$ , and  $K = 1000$ . (a)  $\omega_0/\pi = 0.01$ ,  $\text{SNR} = 40 \text{ dB}$ , and (b)  $\omega_0/\pi = 0.5$ ,  $\text{SNR} = 40 \text{ dB}$ .

Table 3. The results of deviations  $\bar{\Delta}$  [dB] obtained on the basis of data from Fig. 5.

$(\omega_0/\pi)$	$M$	MC-HLA	RPHD-HLA	MPHD-HLA	RC-HLA	ZC	IpDFT-IR
0.01	10÷200	17.8	17.8	12.9	10.9	15.8	30.2
0.01	100÷200	14.2	14.2	7.97	6.27	15.8	21.6
0.5	10÷200	1.40	1.40	1.68	1.58	12.2	9.14
0.5	100÷200	1.38	1.38	1.48	1.47	14.4	9.08

### 3.3. Experimental studies

In order to present the operation of time algorithms in real conditions, measurements were carried out. A sinusoidal voltage with an rms value  $V_{RMS} = 3 \text{ V}$  was generated by an Agilent 33220A function generator. The alternating voltage was sampled using a National Instruments PCI-6024E data acquisition card (Fig. 6). The sampling rate was set  $f_s = 50 \text{ kHz}$ . As a result of the measurements, a file containing  $K = 100$  measurement series was obtained. Each measurement series contained 5000 samples. The SNR was determined for each series. It was obtained that  $\text{SNR} \in [67, 69] \text{ dB}$ . An AIM-TTI TF930 frequency meter was additionally connected to the generator (measurement time was set to 100 seconds). Its task was to measure the reference frequency value  $f_{ref}$  required to determine the estimator errors. In the presented example  $f_{ref} = 49.9984 \text{ Hz}$ . This sinusoidal signal frequency was assumed due to the limited maximum sampling frequency of the measuring card used (200 kS/s) and a greater generator voltage stability in the low frequency range. The standard uncertainty of the frequency measurement was equal to 0.6 ppm and was mainly due to the occurrence of noise in the voltage from the generator (systematic errors of the frequency meter were negligibly small).

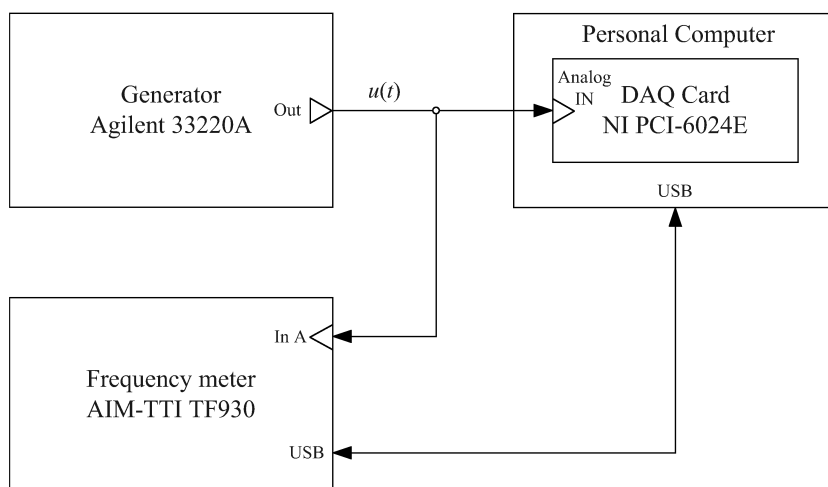


Fig. 6. Block diagram of measurement system.

Based on the obtained data, the MSE charts for the MC-HLA, RPHD-HLA, MPHDLA, ZC, and IpDFT-IR estimators as a function of  $N$  were prepared (Fig. 7). For this purpose, every  $Z$ -th voltage sample was selected from each series. In this way,  $K = 100$  series consisting of  $5000/Z$  voltage samples ( $M = 5000/(2Z)$  samples per period) were obtained. Then, assuming  $z = 1 \dots Z$ , new values  $f_s^{(z)} = f_s/z$ ,  $\omega_0^{(z)} = 2\pi f_{ref}/f_s^{(z)}$ ,  $N^{(z)} = M\omega_0^{(z)}/\pi$  and  $\tilde{R}[y, k]$  were determined. This enabled the estimators calculation and the MSE determination for different  $\omega_0/\pi$  values. The calculations were made for  $Z = 250$  ( $M = 10$ ,  $0 < \omega_0/\pi \leq 0.5$ ,  $0 < N \leq 5$ , Fig. 7a) and  $Z = 25$  ( $M = 100$ ,  $0 < \omega_0/\pi \leq 0.05$ ,  $0 < N \leq 5$ , Fig. 7b). The MSE results were compared with the CRLB calculated on the basis of  $\text{SNR} = 67 \text{ dB}$ . The experimental results confirmed the simulation results. In a situation where  $\text{SNR} \gg 0$ , the RC-HLA estimator was determining the frequency with the highest accuracy.

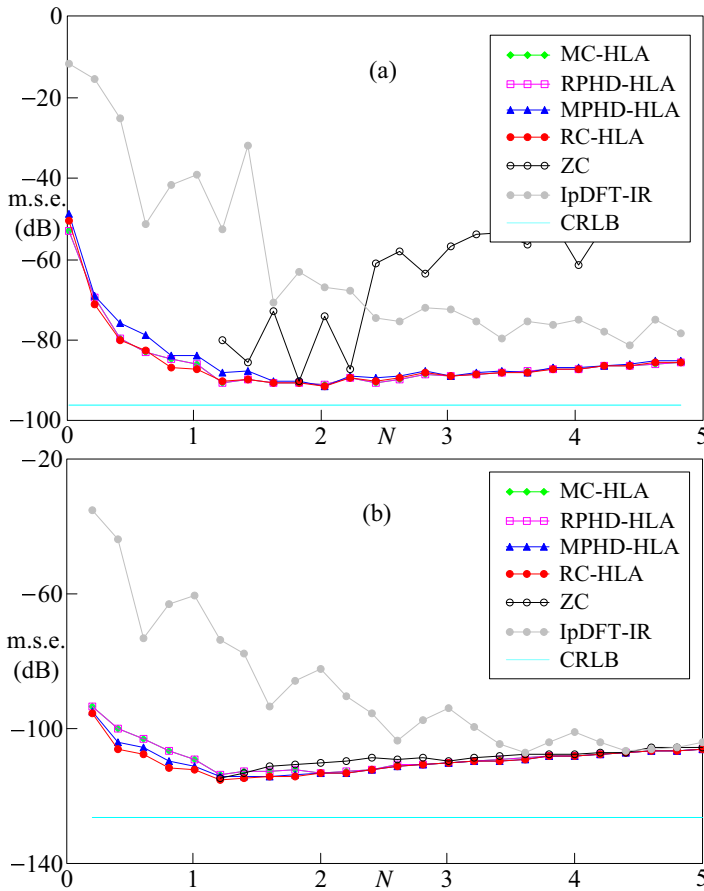


Fig. 7. Results showing the  $\tilde{MSE}$  as a function of  $N$  for  $w = 5$ , and  $K = 100$ . (a)  $0 < \omega_0/\pi \leq 0.5$ ,  $M = 10$ ,  $Z = 250$ , and (b)  $0 < \omega_0/\pi \leq 0.05$ ,  $M = 100$ ,  $Z = 25$ .

### 3.4. Comparison of computational complexity

We analyzed the computational complexity of the RC-HLA estimator. Let RC represent the reformed covariance estimator calculated using formula (17) and samples  $y[n]$  of signal  $y(t)$ . To calculate the RC estimator,  $S = 3M - 8$  additions and  $P = 2M + 2w - 3$  multiplications if  $M \geq 2w + 3$ , or  $P = 4M - 2w - 9$  multiplications if  $M < 2w + 3$  are required. The computational complexity of the RC estimator corresponds to that of the MC estimator ( $S = 3M - 8$ ,  $P = 2M - 3$ ) for  $w = 0$  [12]. The computational complexity of the RC-HLA estimator was determined based on that of the RC estimator. To calculate the RC-HLA,  $S = M^2 + 2M - 8$  additions and  $P = M^2 + 2M + 2w - 3$  multiplications if  $M \geq 2w + 3$ , or  $P = M^2 + 4M - 2w - 9$  multiplications if  $M < 2w + 3$  are required.

Table 4 presents the  $S$  (number of additions/subtractions) and  $P$  (number of multiplication/division) values for the selected estimators which were determined based on the literature [10, 12, 15] and results of our own study. Table 5 presents  $S$  and  $P$  values for the selected  $M$ . The research results have shown that the ZC estimator has the least computational complexity. Moreover, the ZC estimator does not require the calculation of trigonometric functions. If we

consider only the estimators that use the ACF, then the developed estimator is characterized by the smallest number of additions(on a par with the MC-HLA) as well as the largest number of multiplications(the maximum multiplication difference against the best MPHD-HLA algorithm was 11 for  $w = 5$ ). Whereas, the advantage of the RC-HLA and MC-HLA over the RPHD-HLA and MPHD-HLA estimators is that they do not require root square operations. Table 5 shows that the IpDFT-IR estimator requires fewer summations and multiplications than the estimators that use the ACF. However, it should be borne in mind that the formulas developed deal with one iteration of the algorithm(three iterations were assumed in the tests) and do not take into account the calculations that should be made earlier to determine the DFT bin with the maximum magnitude. In addition, compared with the other estimators, the use of the IpDFT-IR requires the calculation of a much larger number of trigonometric functions in operations on real numbers.

Table 4. Computational complexities of the frequency estimators.

Estimator	Addition/ subtraction(S)	Multiplication/division(P)	Square root	Trigonometric functions
RC-HLA	$M^2 + 2M - 8$	$M^2 + 2M + 2w - 3$ if $M \geq 2w + 3$	0	1
		$M^2 + 4M - 2w - 9$ if $M < 2w + 3$		
MC-HLA		$M^2 + 2M - 3$		
RPHD-HLA	$M^2 + 2M - 3$	$M^2 + 2M + 5$	1	
MPHD-HLA	$M^2 + 3M - 16$	$M^2 + 2M - 4$		
ZC*	$5N' + 1$	$2N' + 3$	0	0
IpDFT-IR**	$16M + 3$	$24M + 1$	4	$16M - 8$

\*  $N' = \text{floor}(N) - \text{number of sinusoidal signal periods detected}(N' > 1)$ ,

\*\* Computational complexity deals with one iteration of the algorithm and does not include calculations necessary to determine the DFT bin with the maximum magnitude.

Table 5. The number of additions/subtraction(S) and multiplications/division(P) for the selected  $M$  and for the different frequency estimators.

$M$	RC-HLA( $w = 5$ )		MC-HLA	
	S	P	S	P
10	112	121	112	117
100	10192	10207	10192	10197
	RPHD-HLA		MPHD-HLA	
10	117	125	114	116
100	10197	10205	10284	10196
	ZC		IpDFT-IR(one iteration)	
10	$6 \div 51$	$5 \div 23(1 \leq N' \leq 10)$	163	241
100	$6 \div 501(1 \leq N' \leq 100)$	$5 \div 203$	1603	2401

## 4. Conclusions

In this paper, a new sinusoidal signal frequency estimator based on the signal autocorrelation function(RC-HLA) was presented. The proposed estimator has a simple closed form and high

accuracy. The designed estimator was compared with other estimators such as the MC-HLA, RPHD-HLA, MPHD-HLA, ZC, and IpDFT-IR.

The obtained results have shown that the RC-HLA estimator and the other estimators that use the ACF are more accurate than the popular zero crossing (ZC) estimator and an iterative estimator based on the discrete Fourier transform IpDFT-IR. The largest mean deviations of the MSE from the CRLB for the RC-HLA, MC-HLA, RPHD-HLA, MPHD-HLA, ZC, and IpDFT-IR estimators were respectively equal to 16.4, 22.2, 22.5, 14.7, 59.5, and 24.8 dB, within a wide range of  $0.01 \leq \omega_0/\pi \leq 0.99$  ( $\omega_0/\pi = 2f/f_s$ ,  $1 \leq N \leq 99$ ) and  $-20 < \text{SNR} < 80$  dB. However, in the range of  $0.01 \leq \omega_0/\pi \leq 0.99$  and the narrower range of  $25 < \text{SNR} < 80$  dB, the largest mean deviations of the MSE from the CRLB for the RC-HLA, MC-HLA, RPHD-HLA, MPHD-HLA, ZC and IpDFT-IR estimators were equal to 4.84, 10.6, 10.6, 6.29, 59.5, and 30.6 dB, respectively. The presented results indicate that the RC-HLA and MPHD-HLA estimators are the most accurate because their mean deviations are the smallest. However, the RC-HLA estimator is more accurate than the other estimators for  $\text{SNR} > 25$  dB and  $N < 5$ . In the case of  $\text{SNR} < 25$  dB, preliminary filtering of the signal may be considered. This will result in an increase in the SNR level. The accuracy of frequency estimation will also increase. This applies not only to the developed estimator, but above all to the ZC estimator whose errors were sometimes the greatest.

In summary, the RC-HLA estimator is one of the most accurate estimators that use the ACF. It is characterized by the low computational complexity. In particular, it does not require calculating the square root and using more than one trigonometric function. Its properties, like other ACF-based estimators, indicate the possibility of its use in measurement applications in which the sinusoidal signal in the presence of noise for  $\text{SNR} > 10$  dB is analyzed.

### Acknowledgements

The authors appreciate the constructive comments and suggestions of the anonymous reviewers.

### Appendix

This section derives the formula for the variance of the RC-HLA estimator. This formula has a generalized form for  $M > 13$ . The formulae are different for every other value of  $2 < M \leq 13$  and are thus not presented in this article. We assume  $M > 13$  and  $w = 5$ . Then from (20) and [12] it follows that

$$\text{Var} [\hat{\omega}_0^{\text{RC-HLA}}] = \frac{\text{Var} [\hat{z}]}{\sin^2(\omega_0)}, \tag{31}$$

where

$$\hat{z} = f(\hat{\mathbf{R}}) = \frac{\sum_{k=1}^{M-7} \sum_{n=0}^5 (\tilde{\mathbf{R}}[y, k+n-1] + \tilde{\mathbf{R}}[y, k+n+1]) \tilde{\mathbf{R}}[y, k+n]}{2 \sum_{k=1}^{M-7} \sum_{n=0}^5 \tilde{\mathbf{R}}^2[y, k+n]}, \tag{32}$$

$$\hat{\mathbf{R}} = [\tilde{\mathbf{R}}[y, 0] \dots \tilde{\mathbf{R}}[y, M-1]]^T.$$



From [12] it follows that

$$\text{Var}[\hat{\mathbf{z}}] \approx \mathbf{v}^T \mathbf{D} \mathbf{v}, \tag{33}$$

where  $\mathbf{v} = \nabla f(\hat{\mathbf{R}})|_{\hat{\mathbf{R}}=\tilde{\mathbf{R}}}$ , while  $\mathbf{D}$  is a covariance matrix with size  $M \times M$  and elements

$$d_{k,m} = \begin{cases} \frac{A^2\sigma_q^2}{M} + \frac{\sigma_q^4}{M} + \frac{A^2\sigma_q^2}{M^2}(M-k-1)\cos(2(k-1)\omega_0), & k = m, \\ \frac{A^2\sigma_q^2}{2M^2}((2M-|m-k-1|)\cos((m-k-1)\omega_0) + \\ + (2M-k-m-1)\cos((m+k-1)\omega_0)), & k \neq m, \end{cases} \tag{34}$$

wherein  $k, m = 1 \dots M$ . Formula (34) and its derivation are presented in [12]. The elements on the diagonal of matrix  $\mathbf{D}$  represent the variance  $\text{Var}[\tilde{\mathbf{R}}[y, k]]$  (15), which takes the form shown in formula (34) when  $k = m$  and the component (9) is negligibly small.

The vector  $\mathbf{v}$  can be found by computing the partial derivatives of  $f(\hat{\mathbf{R}})$ . Let us denote:

$$A = \frac{1}{2} \sum_{k=1}^{M-7} \sum_{n=0}^5 (\tilde{\mathbf{R}}[y, k+n-1] + \tilde{\mathbf{R}}[y, k+n+1]) \tilde{\mathbf{R}}[y, k+n], \tag{35}$$

$$B = \sum_{k=1}^{M-7} \sum_{n=0}^5 \tilde{\mathbf{R}}^2[y, k+n]. \tag{36}$$

Evaluating the first seven derivatives of function (32) at  $\tilde{\mathbf{R}}[y, 0] \dots \tilde{\mathbf{R}}[y, 6]$ , we obtain:

$$\begin{aligned} \frac{\partial f}{\partial \tilde{\mathbf{R}}[y, 0]} &= \frac{\tilde{\mathbf{R}}[y, 1]}{2B} = \frac{\cos(\omega_0)}{A^2C}, \\ \frac{\partial f}{\partial \tilde{\mathbf{R}}[y, 1]} &= \frac{\tilde{\mathbf{R}}[y, 0] + 3\tilde{\mathbf{R}}[y, 2]}{2B} - \frac{2A}{B^2} \tilde{\mathbf{R}}[y, 1] = \frac{\tilde{\mathbf{R}}[y, 0] + 3\tilde{\mathbf{R}}[y, 2]}{2B} - \frac{2\tilde{\mathbf{R}}[y, 1] \cos(\omega_0)}{B} \\ &= \frac{1 + 3 \cos(2\omega_0) - 4 \cos(\omega_0) \cos(\omega_0)}{A^2C}, \\ &\vdots \\ \frac{\partial f}{\partial \tilde{\mathbf{R}}[y, 6]} &= \frac{11\tilde{\mathbf{R}}[y, 5] + 12\tilde{\mathbf{R}}[y, 7]}{2B} - \frac{12A}{B^2} \tilde{\mathbf{R}}[y, 6] \\ &= \frac{11 \cos(5\omega_0) + 12 \cos(7\omega_0) - 24 \cos(6\omega_0) \cos(\omega_0)}{A^2C}, \end{aligned} \tag{37}$$

where

$$C = \sum_{k=1}^{M-7} \sum_{n=0}^5 \cos^2(k+n) \approx 3M - 21. \tag{38}$$

Similarly, evaluating the last seven derivatives of function (32) at  $\tilde{R}[y, M - 7] \dots \tilde{R}[y, M - 1]$ , we obtain:

$$\begin{aligned} \frac{\partial f}{\partial \tilde{R}[y, M - 1]} &= \frac{\tilde{R}[y, M - 1]}{2B} = \frac{\cos((M - 1)\omega_0)}{A^2C}, \\ \frac{\partial f}{\partial \tilde{R}[y, M - 2]} &= \frac{\tilde{R}[y, M - 1] + 3\tilde{R}[y, M - 3]}{2B} - \frac{4A}{B^2}\tilde{R}[y, M - 2] \\ &= \frac{3 \cos((M - 3)\omega_0) + \cos((M - 1)\omega_0) - 8 \cos((M - 2)\omega_0) \cos(\omega_0)}{A^2C}, \\ &\vdots \\ \frac{\partial f}{\partial \tilde{R}[y, M - 7]} &= \frac{12\tilde{R}[y, M - 8] + 11\tilde{R}[y, M - 6]}{2B} - \frac{12A}{B^2}\tilde{R}[y, M - 7] \\ &= \frac{12 \cos((M - 8)\omega_0) + 11 \cos((M - 6)\omega_0) - 24 \cos((M - 7)\omega_0) \cos(\omega_0)}{A^2C}. \end{aligned} \tag{39}$$

It can be shown that the derivatives of function (32) calculated at  $\tilde{R}[y, 7] \dots \tilde{R}[y, M - 8]$  equal zero, *i.e.*

$$\frac{\partial f}{\partial \tilde{R}[y, 7]} = \dots = \frac{\partial f}{\partial \tilde{R}[y, M - 8]} = 0. \tag{40}$$

For example,

$$\begin{aligned} \frac{\partial f}{\partial \tilde{R}[y, 7]} &= \frac{12\tilde{R}[y, 6] + 12\tilde{R}[y, 8]}{2B} - \frac{12A}{B^2}\tilde{R}[y, 7] \\ &= \frac{12 \cos(6\omega_0) + 12 \cos(8\omega_0) - 24 \cos(7\omega_0) \cos(\omega_0)}{A^2C}, \\ \frac{\partial f}{\partial \tilde{R}[y, M - 8]} &= \frac{12\tilde{R}[y, M - 9] + 12\tilde{R}[y, M - 7]}{2B} - \frac{12A}{B^2}\tilde{R}[y, M - 8] \\ &= \frac{12 \cos((M - 9)\omega_0) + 12 \cos((M - 7)\omega_0) - 24 \cos((M - 8)\omega_0) \cos(\omega_0)}{A^2C}. \end{aligned} \tag{41}$$

As for any  $\omega_0$ , the formulas

$$\begin{aligned} 12 \cos(6\omega_0) + 12 \cos(8\omega_0) - 24 \cos(7\omega_0) \cos(\omega_0) &= 0, \\ 12 \cos((M - 9)\omega_0) + 12 \cos((M - 7)\omega_0) - 24 \cos((M - 8)\omega_0) \cos(\omega_0) &= 0, \end{aligned} \tag{42}$$

then

$$\frac{\partial f}{\partial \tilde{R}[y, 7]} = \frac{\partial f}{\partial \tilde{R}[y, M - 8]} = 0. \tag{43}$$

Based on (38)–(43), we can obtain

$$\mathbf{v} = \frac{\mathbf{h}}{3A^2(M - 7)}, \tag{44}$$

where  $\mathbf{h}$  is a vector with size  $M \times 1$  and elements  $h_i, i = 1 \dots M$ , described by formula:

$$h_i = \begin{cases} \cos(\omega_0) & i = 1, \\ 1 + 3 \cos(2\omega_0) - 4 \cos(\omega_0) \cos(\omega_0) & i = 2, \\ 3 \cos(\omega_0) + 5 \cos(3\omega_0) - 8 \cos(2\omega_0) \cos(\omega_0) & i = 3, \\ 5 \cos(2\omega_0) + 7 \cos(4\omega_0) - 12 \cos(3\omega_0) \cos(\omega_0) & i = 4, \\ 7 \cos(3\omega_0) + 9 \cos(5\omega_0) - 16 \cos(4\omega_0) \cos(\omega_0) & i = 5, \\ 9 \cos(4\omega_0) + 11 \cos(6\omega_0) - 20 \cos(5\omega_0) \cos(\omega_0) & i = 6, \\ 11 \cos(5\omega_0) + 12 \cos(7\omega_0) - 24 \cos(6\omega_0) \cos(\omega_0) & i = 7, \\ 12 \cos((M-8)\omega_0) + 11 \cos((M-6)\omega_0) - 24 \cos((M-7)\omega_0) \cos(\omega_0) & i = M-6, \\ 11 \cos((M-7)\omega_0) + 9 \cos((M-5)\omega_0) - 20 \cos((M-6)\omega_0) \cos(\omega_0) & i = M-5, \\ 9 \cos((M-6)\omega_0) + 7 \cos((M-4)\omega_0) - 16 \cos((M-5)\omega_0) \cos(\omega_0) & i = M-4, \\ 7 \cos((M-5)\omega_0) + 5 \cos((M-3)\omega_0) - 12 \cos((M-4)\omega_0) \cos(\omega_0) & i = M-3, \\ 5 \cos((M-4)\omega_0) + 3 \cos((M-2)\omega_0) - 8 \cos((M-3)\omega_0) \cos(\omega_0) & i = M-2, \\ 3 \cos((M-3)\omega_0) + \cos((M-1)\omega_0) - 4 \cos((M-2)\omega_0) \cos(\omega_0) & i = M-1, \\ \cos((M-2)\omega_0) & i = M, \\ 0 & \text{elsewhere.} \end{cases} \quad (45)$$

Substituting (44) into (33) and then (33) into (31), we obtain

$$\text{Var} \left[ \tilde{\omega}_0^{\text{RC-HLA}} \right] \approx \frac{\mathbf{h}^T \mathbf{D} \mathbf{h}}{9A^4(M-7)^2 \sin^2(\omega_0)}. \quad (46)$$

As  $\tilde{\omega}_0^{\text{RC-HLA}}$  is asymptotically unbiased (the estimator's bias tends to zero as  $M$  increases [27]), then

$$\text{MSE} \left[ \tilde{\omega}_0^{\text{RC-HLA}} \right] \approx \text{Var} \left[ \tilde{\omega}_0^{\text{RC-HLA}} \right] = \frac{\mathbf{h}^T \mathbf{D} \mathbf{h}}{9A^4(M-7)^2 \sin^2(\omega_0)}. \quad (47)$$

## References

- [1] Al-Qudsi, B., El-Shennawy, M., Joram, N., Ellinger, F. (2017). Enhanced zero crossing frequency estimation for FMCW radar systems. *Proc. of the 13th Conference on Ph. D. Research in Microelectronics and Electronics (PRIME)*, Giardini Naxos, Italy, 53–56.
- [2] Hague, D.A., Buck, J.R. (2019). An experimental evaluation of the generalized sinusoidal frequency modulated waveform for active sonar systems. *Journal of the Acoustical Society of America*, 145(6), 3741–3755.
- [3] Rice, F., Cowley, B., Moran, B., Rice, M. (2001). Cramér–Rao lower bounds for QAM phase and frequency estimation. *IEEE Transactions on Communications*, 49(9) 1582–1591.
- [4] Toth, L., Kocsor, A. (2003). Harmonic alternatives to sine-wave speech. *Proc. of the 8th European Conference on Speech Communication and Technology*, Geneva, Switzerland, 2073–2076.
- [5] Adelson, R.M. (1997). Frequency estimation from few measurements. *Digital Signal Processing*, 7(1), 47–54.

- [6] Vizireanu, D.N. (2012). A fast, simple and accurate time-varying frequency estimation method for single-phase electric power systems. *Measurement*, 45(5), 1331–1333.
- [7] Pan, X., Zhao, H., Zou, W., Zhou, Y., Ma, J., Wang, J., Hu, F. (2016). Frequency estimation of discrete time signals based on fast iterative algorithm. *Measurement*, 82, 461–465.
- [8] Pei, D., Xia, Y. (2019). Robust power system frequency estimation based on a sliding window approach. *Mathematical Problems in Engineering*, 2019, 3254258.
- [9] Sienkowski, S., Krajewski, M. (2018). Simple, fast and accurate four-point estimators of sinusoidal signal frequency. *Metrology and Measurement Systems*, 25(2), 359–376.
- [10] Elasmî-Ksibi, R., Besbes, H., López-Valcarce, R., Cherif, S. (2010). Frequency estimation of real-valued single-tone in colored noise using multiple autocorrelation lags. *Signal Processing*, 90(7), 2303–2307.
- [11] Cao, Y., Wei, G., Chen, F.J. (2012). An exact analysis of modified covariance frequency estimation algorithm based on correlation of single-tone. *Signal processing*, 92(11), 785–2790.
- [12] Martinez, M.A., Ashrafi, A. (2018). Real-valued single-tone frequency estimation using half-length autocorrelation. *Digital Signal Processing*, 83, 98–106.
- [13] So, H.C. (2002). A closed form frequency estimator for a noisy sinusoid. *Proc. of the 45th Midwest Symposium on Circuits and Systems(MWSCAS-2002)*, 2, Tulsa, USA, 160–163.
- [14] Lui, K.W.K., So, H.C. (2008). Modified Pisarenko harmonic decomposition for single-tone frequency estimation. *IEEE Transactions on Signal Processing*, 56(7), 3351–3356.
- [15] Elasmî-Ksibi, R., López-Valcarce, R., Besbes, H., Cherif, S. (2008). A family of real single-tone frequency estimators using higher-order sample covariance lags. *Proc. of the 16th European Signal Processing Conference*, Lausanne, Switzerland.
- [16] Tu, Y.Q., Shen, Y.L. (2017). Phase correction autocorrelation-based frequency estimation method for sinusoidal signal. *Signal Processing*, 130, 183–189.
- [17] Duda, K., Zielinski, T.P. (2013). Efficacy of the frequency and damping estimation of a real-value sinusoid Part 44 in a series of tutorials on instrumentation and measurement. *IEEE Instrumentation & Measurement Magazine*, 16(2), 48–58.
- [18] Eriksson, A., Stoica, P. (1993). On statistical analysis of Pisarenko tone frequency estimator. *Signal Processing*, 31(3), 349–353.
- [19] Phadke, A.G., Thorp, J.S., Adamiak, M.G. (1983). A new measurement technique for tracking voltage phasors, local system frequency, and rate of change of frequency. *IEEE Transactions on Power Apparatus and Systems*, PAS-102(5), 1025–1038.
- [20] Borkowski, J., Kania, D., Mroczka, J. (2018). Comparison of sine-wave frequency estimation methods in respect of speed and accuracy for a few observed cycles distorted by noise and harmonics. *Metrology and Measurement Systems*, 25(2), 283–302
- [21] Duda, K. (2012). Interpolation Algorithms of DFT for parameters estimation of sinusoidal and damped sinusoidal signals. *Fourier Transform-Signal Processing*. InTech – Open Access Publisher.
- [22] Serbes, A. (2018). Fast and efficient sinusoidal frequency estimation by using the DFT coefficients. *IEEE Transactions on Communications*, 67(3), 2333–2342.
- [23] Ye, S., Sun, J., Aboutanios, E. (2017). On the estimation of the parameters of a real sinusoid in noise. *IEEE Signal Processing Letters*, 24(5), 638–642.
- [24] Djukanović, S., Popović-Bugarin, V. (2019). Efficient and accurate detection and frequency estimation of multiple sinusoids. *IEEE Access*, 7, 1118–1125.
- [25] Candan, Ç. (2015). Fine resolution frequency estimation from three DFT samples: Case of windowed data. *Signal Processing*, 114, 245–250.

- [26] Belega, D., Petri, D., Dallet, D. (2018). Accurate frequency estimation of a noisy sine-wave by means of an interpolated discrete-time Fourier transform algorithm. *Measurement*, 116, 685–691.
- [27] Bendat, J.S., Piersol, A.G. (2010). *Random Data: Analysis and Measurement Procedures*. 4th ed. USA: John Wiley & Sons.
- [28] Lal-Jadziak, J., Sienkowski, S. (2009). Variance of random signal mean square value digital estimator. *Metrology and Measurement Systems*, 16(2), 267–278.
- [29] Benaroya, H., Mi Han, S., Nagurka, M. (2005). *Probability Models in Engineering and Science*. CRC Press.
- [30] Fessler, J. (2015). Chapter 23 Mean and Variance Analysis. In *Image reconstruction: Algorithms and analysis*, Book draft, <https://web.eecs.umich.edu/~fessler/book/c-mav.pdf> (accessed on Aug. 2020).
- [31] Kay, S.M. (1993). *Fundamentals of Statistical Signal Processing: Estimation Theory*, Englewood Cliffs. New Jersey: Prentice-Hall.